doi:10.1016/j.jmb.2008.05.008 J. Mol. Biol. (2008) 380, 373–385

JMB

Available online at www.sciencedirect.com

ScienceDirect

ELSEVIER

Substrate recognition by family 7 alginate lyase from *Sphingomonas* sp. A1

Kohei Ogura[1], Masayuki Yamasaki[2], Bunzo Mikami[2], Wataru Hashimoto[1] and Kousaku Murata[1]*

[1]*Division of Food Science and Biotechnology, Graduate School of Agriculture, Kyoto University, Uji, Kyoto 611-0011, Japan*

[2]*Division of Applied Life Sciences, Graduate School of Agriculture, Kyoto University, Uji, Kyoto 611-0011, Japan*

Received 3 December 2007; received in revised form 2 May 2008; accepted 7 May 2008
Available online 11 May 2008

Sphingomonas sp. A1 alginate lyase A1-II′, a member of polysaccharide lyase family 7, shows a broad substrate specificity acting on poly α-L-guluronate (poly(G)), poly β-D-mannuronate (poly(M)) and the heteropolymer (poly (MG)) in alginate molecules. A1-II′ with a glove-like β-sandwich as a basic scaffold forms a cleft covered with two lid loops (L1 and L2). Here, we demonstrate the loop flexibility for substrate binding and structural determinants for broad substrate recognition and catalytic reaction. The two loops associate mutually over the cleft through the formation of a hydrogen bond between their edges (Asn141 and Asn199). A double mutant, A1-II′ N141C/N199C, has a disulfide bond between Cys141 and Cys199, and shows little enzyme activity. Adding dithiothreitol to the enzyme reaction mixture leads to a tenfold increase in its molecular activity, suggesting the significance of flexibility in lid loops for accommodating the substrate into the active cleft. In alginate trisaccharide (GGG or MMG)-bound A1-II′ Y284F, the enzyme interacts appropriately with substrate hydroxyl groups at subsites +1 and +2 and accommodates G or M, while substrate carboxyl groups are strictly recognized by specific residues. This mechanism for substrate recognition enables A1-II′ to show the broad substrate specificity. The structure of A1-II′ H191N/Y284F complexed with a tetrasaccharide bound at subsites −1 to +3 suggests that Gln189 functions as a neutralizer for the substrate carboxyl group, His191 as a general base, and Tyr284 as a general acid. This is, to our knowledge, the first report on the structure and function relationship in family 7.

Keywords: alginate; polysaccharide lyase; X-ray crystallography; substrate specificity; catalytic mechanism

Edited by G. Schulz

Introduction

Alginate is a linear polysaccharide composed of α-L-guluronate (G) and its C5 epimer β-D-mannuronate (M), and arranged in three regions: poly(G), poly(M), and heteropolymeric random sequences (poly(MG)) (Fig. 1).[1] The polysaccharide is produced by certain bacteria and brown seaweed. Opportunistic pathogens such as *Pseudomonas aeruginosa* produce extracellular biofilms including alginate as important virulence factors during lung infections in cystic fibrosis patients.[2] These biofilms often protect

*Corresponding author. E-mail address: kmurata@kais.kyoto-u.ac.jp.

Abbreviations used: rmsd, root-mean-square deviation; G, α-L-guluronate; M, β-D-mannuronate; strain A1, *Sphingomonas* sp. A1; A1-I, strain A1 alginate lyase I; A1-II, strain A1 alginate lyase II; A1-III, strain A1 alginate lyase III; A1-IV, strain A1 alginate lyase IV; A1-IV′, strain A1 alginate lyase IV′; A1-II′, strain A1 alginate lyase II′; PA1167, *Pseudomonas aeruginosa* alginate lyase; Aly-PG, *Corynebacterium* sp. α-L-guluronate lyase; MD, molecular dynamics; N141C/N199C, A1-II′ mutant with Asn141 and Asn199 substituted with Cys; DTNB, 5,5′-thiobis-2-nitrobenzonic acid; Y284F, A1-II′ mutant with Tyr284 substituted with Phe; H191N/Y284F, A1-II′ mutant with His191 and Tyr284 substituted with Asn and Phe; DSC, differential scanning calorimetry; PEG, polyethylene glycol; AALyase, *Pseudoalteromonas* sp. alginate lyase; R146A, A1-II′ mutant with Arg146 substituted with Ala; H191A, A1-II′ mutant with His191 substituted with Ala; Hepes, 4-(2-hydroxyethyl)-1-piperazineethanesulfonic acid.

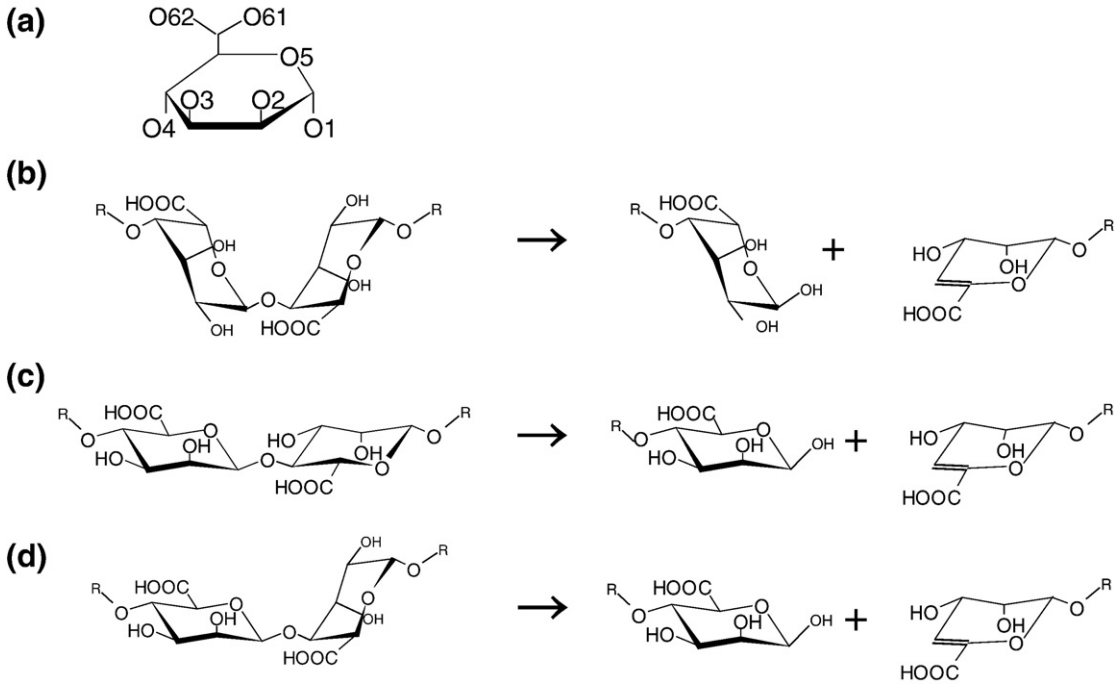

Fig. 1. Alginate and lyase reaction. (a) Haworth projection of M. O1, O2, O3, and O4 are hydroxyl groups. O61 and O62 are arranged in a carboxyl group; (b) poly(G); (c) poly(M); and (d) poly(MG). The arrow indicates the reaction catalyzed by alginate lyases. These pictures were drawn with ChemSketch (http://www.acdlabs.com).

P. aeruginosa cells from phagocytic cells and/or antibiotics, making biofilm-dependent diseases difficult to treat. Bacterial alginate is frequently acetylated in the poly(M) region.[3–5] Alginate from brown seaweed is, in contrast, widely used in the food and pharmaceutical industries because the polymer, especially the poly(G) region, chelates metal ions and forms a highly viscous solution.[6] Oligosaccharides derived from brown seaweed alginate act physiologically as bifidus factors, elicitors of plant growth, enhancers of human endothelial cell and keratinocyte growth, and inducers of cytokine production from mouse macrophage cells.[7–12] Alginate-depolymerizing enzymes are thus expected to become promising as biochemicals for removing bacterial biofilm alginate and processing edible seaweed alginate.[13]

Sphingomonas sp. A1 (strain A1) is a potent producer of alginate-depolymerizing enzymes (alginate lyases).[14] Alginate lyase catalyzes the cleavage of glycosidic bonds in alginate molecules through a β-elimination reaction (Fig. 1). Four types of alginate lyase, A1-I (65 kDa), A1-II (25 kDa), A1-III (40 kDa), and A1-IV (86 kDa), are present in bacterial cytoplasm.[15] Two genes coding for A1-II′ (32 kDa) and A1-IV′ (90 kDa) are included in the bacterial genome, although their expression has not been detected in bacterial cells.[15,16] These six enzymes are categorized into polysaccharide lyase families 5, 7, or 15 in the Carbohydrate Active enZYme database on the basis of their primary structures,[17] and differ in specific activity, substrate specificity (poly(G) poly(M), and/or poly(MG)), and mode of action (*endo* or *exo*). Since, among them, the truncated A1-II′ (25 kDa, Pro81-His316) exhibits endolytical reaction and broad substrate specificity (active on poly(G), poly(M), and poly(MG)), A1-II′ is one of the most promising enzymes for alginate degradation and modification.[16]

The structure and function relationships of alginate lyases, i.e. structural determinants for recognizing G, M, or acetylated M and cleaving glycosidic bonds through β-elimination, must be clarified to establish a basis for the optimal molecular design of the enzymes for food, agricultural, chemical, and/or medical areas. The information on structure and function helps to lower antigenicity of the enzymes as therapeutic agents for bacterial biofilm-dependent diseases, and to produce alginates and their oligosaccharides with different degrees of polymerization and G/M composition. Earlier, we demonstrated the structure and function of family 5 A1-III (PDB ID 1QAZ), which acts specifically on poly(M).[18–20] We have also recently determined the first crystal structures of family 7 alginate lyases, strain A1 A1-II′ (PDB ID 2CWS) and *P. aeruginosa* PA1167 (PDB ID 1VAV).[21,22] The structure of *Corynebacterium* sp. α-L-guluronate lyase Aly-PG (PDB ID 1UAI) belonging to family 7 has also been clarified.[23] These structural analyses indicate that a common basic frame, i.e. a β-sandwich with a deep cleft, exists among family 7 enzymes. Two loops are located over the cleft. These enzymes complexed with ligands such as substrates and/or products have not, however, been structurally analyzed. Little information on the structure and function relationship of family 7 enzymes is available.

A1-II′ is characteristic, in that the enzyme can act on poly(G), poly(M), and poly(MG), although most alginate lyases are specific to one of the three regions. This suggests that A1-II′ has an active site

with binding ability to both G and M. X-ray crystallography of A1-II′ complexed with oligosaccharides derived from poly(G) and poly(M) contributes to the elucidation of structural determinants for broad substrate specificity.

To clarify the structure—function relationship of family 7 alginate lyases, we focused on identifying the loop movement responsible for substrate binding in A1-II′ and its active cleft using X-ray crystallography and site-directed mutagenesis.

Results and Discussion

N141C/N199C crystal structure

A1-II′ in a truncated form (Pro81-His312) shows a glove-like β-sandwich structure composed of four short α-helices and two β-sheets.[21] β-Strands A2 (SA2, residues 94–97), A3 (SA3, 146–152), A4 (SA4, 277–285), and A5 (SA5, 184–191) constitute a cleft. Two loops (L1, 133–145 and L2, 193–203) are located over the cleft. In two kinds of ligand-free A1-II′ structures (PDB ID 2CWS and 2Z42) determined from crystals formed under different crystallization conditions, the positions of L1 are different, i.e. open form (PDB ID 2CWS) and closed form (PDB ID 2Z42). In the closed form, an interaction between L1 and L2 occurs at their tips through hydrogen bond formation between Asn141 and Asn199. Additionally, *B*-factors for L1 and L2 in A1-II′ are quite high.[21] Although family 7 PA1167 and Aly-PG also have loops corresponding to L1 and L2, the loop conformation is different among the three,[21–23] suggesting that these loops oscillate flexibly.

The loop flexibility was confirmed *in silico* by programs GlobPlot[24] and GROMACS.[25] Based on the primary structure, GlobPlot predicts the disordered regions at residues 127–144, 156–164, 194–202, 217–231, 285–291, and 300–308. Most of the putative globular regions other than the disordered regions constitute α or β structural elements in the crystal structure of A1-II′, suggesting that the GlobPlot analysis is reliable for protein disorder and globularity. The disordered regions 127–144 and 194–202 almost correspond to L1 and L2, respectively. Molecular dynamics (MD) simulation by GROMACS reveals the flexibility of the loops. L1 and L2 repeat oscillation in the trajectory of the simulation in length of 1 ns (0.002 ps × 500,000 steps) as follows: C^{α} atoms of Asn141 in L1 and Ala200, a neighbor of Asn199, in L2 are oscillated in range of 3.3 Å and 2.6 Å, respectively, while slight oscillation (less than 1.0 Å) occurs at hinge regions of the loops (L1, Pro133 and Pro145; L2, Ile193 and Leu203). Family 5 alginate lyase A1-III and family 8 chondroitin and hyaluronate lyases were shown to have flexible loops involved in substrate binding and/or catalytic reaction.[19,26,27] The loop flexibility may therefore be shared by family 7 enzymes and important for enzyme activity.

To clarify the significance of the flexibility and interaction of the two loops, we constructed the mutant N141C/N199C with Asn141 and Asn199 replaced by cysteine residues to introduce a rigid interaction between L1 and L2 loops by forming a disulfide bond. The amount of free thiol groups in the mutant was determined by chemical modification assay with 5,5′-thiobis-2-nitrobenzonic acid (DTNB)[28] to examine the disulfide bond formation between Cys141 and Cys199 in N141C/N199C in the absence of a reducing agent. There are only two Cys residues (Cys141 and Cys199) in N141C/N199C. Based on the standard calibration curve prepared with dithiothreitol (DTT), the ratio of the molecules having free thiol groups was determined to be 2.6% in the absence of DTT. This result indicates that almost all (97.4%) molecules of N141C/N199C form a disulfide bond between Cys141 and Cys199.

The crystal structure of N141C/N199C (Fig. 2a) was determined at 2.1 Å resolution by X-ray crystallography. Data collection and refinement statistics are shown in Table 1. The mutant has a glove-like β-sandwich structure composed of four short α-helices and two β-sheets. Two sulfate ions derived from the crystallization solution are accommodated at subsites +1 and +3. The root-mean-square deviations (rmsds) between N141C/N199C and the ligand-free wild-type enzyme (PDB ID 2CWS) were observed in C^{α} atoms for the loops (0.67 Å) and the rest (0.49 Å), indicating that no significant conformational change occurs between the two enzymes except their loops. The loops of the mutant adopt the closed form. As expected, a disulfide bond between Cys141 and Cys199 forms in the absence of reducing agents (Fig. 2b). The *B*-factors for the L1 and L2 loops in the mutant are much lower than those in the ligand-free form (PDB ID 2CWS), suggesting that rigid interaction between L1 and L2 loops forms in the mutant in the absence of reducing agents.

Physical properties of N141C/N199C

To evaluate the rigidity of the loop interaction in N141C/N199C, we measured the transition temperature by differential scanning calorimetry (DSC). The transition temperature of the wild-type enzyme was determined to be 45 °C regardless of the presence or the absence of DTT. In the case of N141C/N199C, the transition temperature in the absence of DTT shifted higher than that in the presence of DTT. N141C/N199C in the absence of DTT began to unfold at a higher temperature of 51 °C. The addition of DTT at 0.5 mM final concentration reduced the transition temperature to the same level (45 °C) as that of the wild-type enzyme, indicating that a disulfide bond forms between Cys141 and Cys199 in the mutant in the absence of DTT, thus contributing to the more stable form, and that 0.5 mM DTT is sufficient to prevent the formation of the disulfide bond between Cys141 and Cys199.

Enzymatic properties of N141C/N199C

To clarify the effects of the loop interaction on enzyme activity, we assayed the wild-type and mutant enzymes in the presence and in the absence

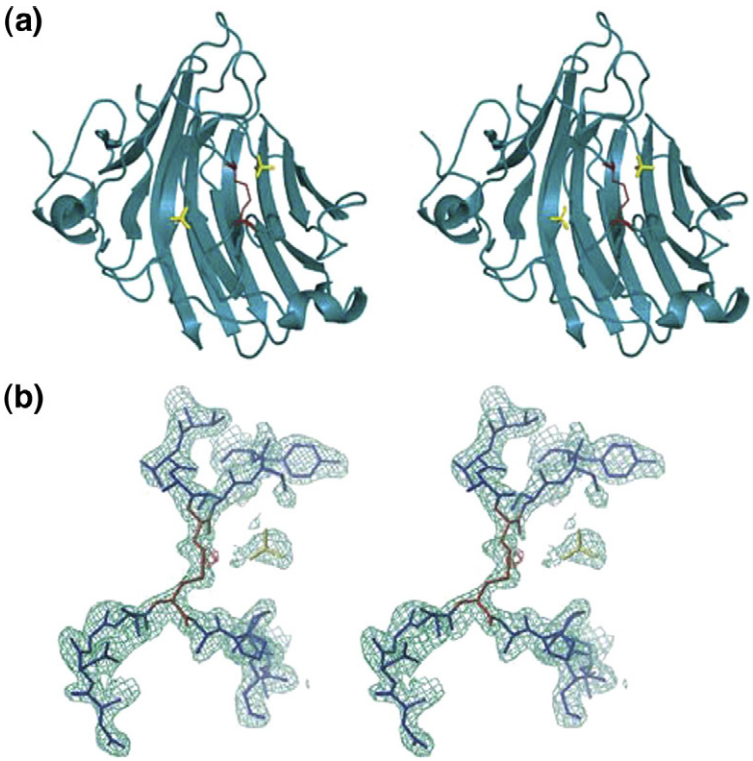

Fig. 2. Structure of N141C/N199C (stereo diagram). (a) Overall structure: red, Cys141 and Cys199; yellow, sulfate ions. (b) Electron density map around the disulfide bond. Green mesh, $2F_o - F_c$ contoured at 1.0 σ; red mesh, $F_o - F_c$ contoured at –3.0 σ. A stick model indicates amino acid residues. Red, Cys141 and Cys199; blue, amino acids around the disulfide bond; yellow, sulfate ions. These pictures were drawn with Pymol (http://www.pymol.org).

of 0.5 mM DTT (Table 2). The kinetic parameters K_m and V_{max} of these enzymes in the absence of DTT toward alginate were 0.018 mg/ml and 42.9 U/mg, respectively, for the wild-type enzyme, and 0.14 mg/ml and 0.63 U/mg, respectively, for the mutant. In the presence of DTT, K_m and V_{max} of the mutant were 0.32 mg/ml and 7.1 U/mg, respectively. No change in the activity of the wild-type enzyme was observed in the presence or in the absence of DTT. In the absence of DTT, V_{max} of the mutant corresponded to

Table 1. Data collection, structure refinement, and model status of complexes

	N141C/N199C	Y284F-GGG	Y284F-MMG	H191N/Y284F-GGMG
A. *Data collection*				
Cell dimensions				
a (Å)	35.460	34.73	34.94	43.70
b (Å)	70.61	68.10	68.88	60.82,
c (Å)	90.73	79.95	80.43	75.04
Space group	$P2_12_12_1$	$P2_12_12_1$	$P2_12_12_1$	$P2_12_12_1$
Molecules/asymmetric unit	1	1	1	1
Resolution range (last shell)	50–2.10 (2.18–2.10)	50–1.65 (1.71–1.65)	50–1.50 (1.55–1.50)	50–1.8 (1.86–1.80)
Reflections (last shell)	70,105 (6395)	136,401 (10,515)	268,545 (10,621)	168,714 (16,339)
Completeness (%) (last shell)	95.5 (93.8)	97.7 (95.6)	96.3 (74.1)	100 (100)
Average I/σ (last shell)	24.6 (3.4)	56.7 (5.9)	20.8 (4.4)	29.2 (5.5)
$R(I)_{merge}$ (%) (last shell)	7.3 (30.5)	4.3 (19.7)	4.8 (22.6)	5.7 (27.6)
B. *Structure refinement*				
Resolution range	15–2.10	50–1.65	50–1.55	15.0–1.8
R-factor (R_{cryst} / R_{free})	18.9/23.7	18.8/21.6	16.7/18.1	16.9/19.8
C. *Model status*				
rmsd from ideal values				
Bond lengths (Å)	0.006	0.005	0.17	0.005
Bond angles (deg.)	1.39	1.402	6.973	1.11
Ramachandran plot				
Most favored regions (%)	85	88.5	88.1	87.4
Additionally allowed regions (%)	14.4	11.5	11.9	12.6
Generally allowed regions (%)	0.5	0	0	0
Disallowed regions (%)	0	0	0	0
Molecules/Average *B*-factor (Å^2)				
Amino acid residues	232[a]/11.44	226[b]/14.84	227[c]/10.15	232[a]/26.03
Water molecules	153/21.59	214/31.91	277/32.37	129/30.32
Saccharides	–	1/40.66	1/36.83	1/21.91

[a]Pro81-His312, [b]Ala82-Ser307, and [c]Pro81-Ser307 are observed in these models.

Table 2. Kinetic parameters of wild-type and mutant enzymes

Enzyme	Addition	K_m (mg/ml)	V_{max} (U/mg)	Relative V_{max}/K_m (%)
Wild-type	–	0.018	42.9	100
N141C/N199C	0.5 mM DTT	0.32	7.1	0.96
N141C/N199C	–	0.14	0.63	0.19

1.5% although K_m corresponded to 7.8-fold compared to the counterparts of the wild-type enzyme, while V_{max} corresponded to 17% and K_m corresponded to 17.7-fold in the presence of DTT. The low affinity (increased K_m) and activity (decreased V_{max}) of the mutant is probably due to mutations in which Asn141 and Asn199 are replaced by cysteine residues, because these Asn residues are involved in binding to substrates through the formation of hydrogen bonds, and these interactions have a significant effect on the enzyme activity, as described later. V_{max} of the mutant in the presence of DTT was 11.3-fold higher than that in the absence of DTT, indicating directly that the rigid interaction in loops L1 and L2 inhibits the access of substrates to the

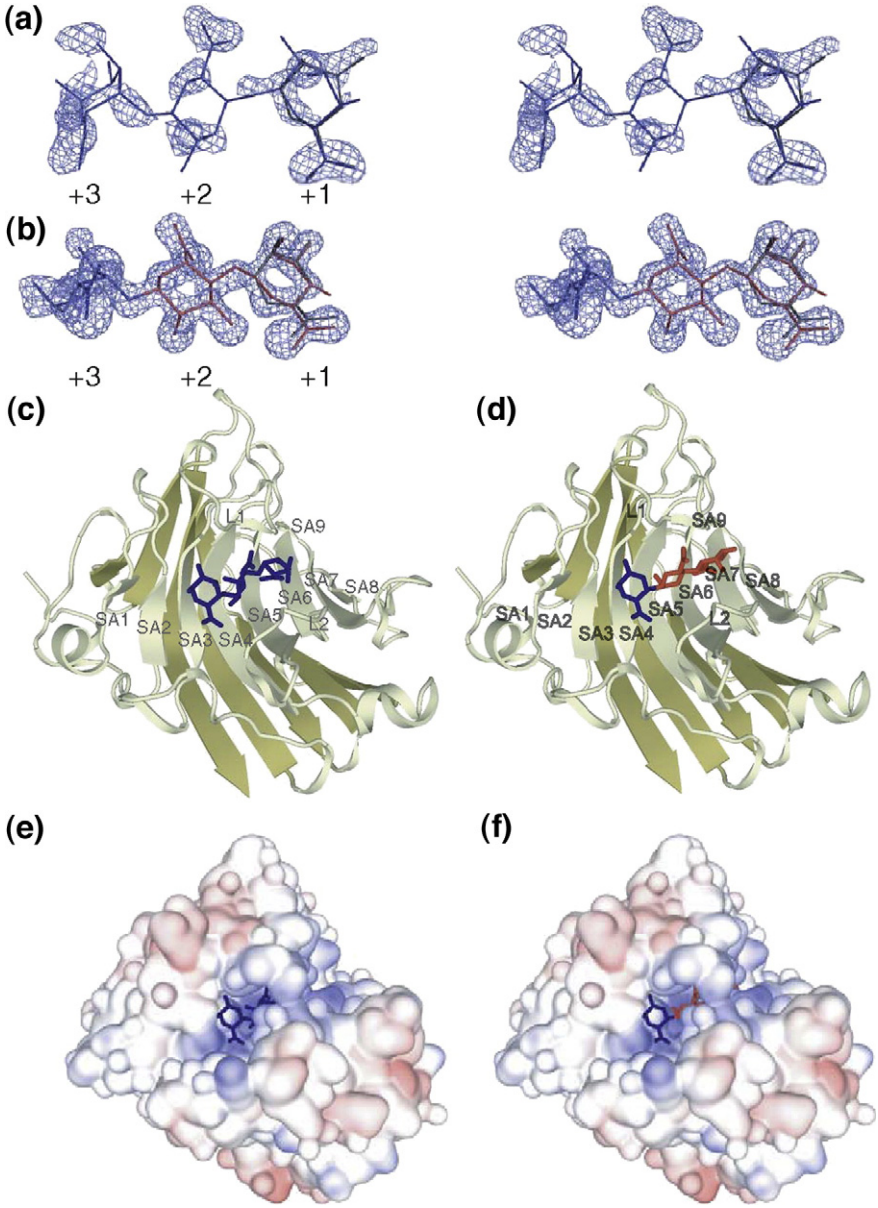

Fig. 3. Structures of trisaccharide-bound Y284Fs. (a) The F_o-F_c omit map for GGG (blue, contoured at 3.0 σ) (stereo diagram): blue, G; black, unsaturated uronic acid. (b) The F_o-F_c omit map for MMG (blue, contoured at 3.0 σ) (stereo diagram): red, M; blue, G; black, unsaturated uronic acid. (c) The overall structure of GGG-bound Y284F. The trisaccharide is shown as a stick model (blue, G). Secondary structural elements are indicated (SA1-9, β-strand; L1-2, loop). (d) The overall structure of MMG-bound Y284F. The trisaccharide is shown by sticks (blue, G; red, M). (e and f) The molecular surfaces of GGG-bound Y284F (e) and MMG-bound Y284F (f). The trisaccharide is shown as a stick model (blue, G; red, M). Blue and red on surfaces indicate positively and negatively charged residues, respectively. a, b and c–f were drawn with Pymol (http://www.pymol.org) and MolFeat (FiatLux).

active site. A1-II′ is known to show endolytic activity, meaning that the enzyme repeatedly allows an access of substrates to the active site and a release of products from the site.[16] Flexibility in loops L1 and L2 of A1-II′ is therefore essential for the repeat of the access and release.

Crystal structures of trisaccharide-bound Y284F

Crystal structures of the wild-type enzyme (PDB IDs 2CWS and 2Z42) contain two sulfate ions derived from the crystallization solution in the deep cleft, making it difficult to determine the structure of the enzyme–substrate complex.[21] Sulfate ions competitively inhibit A1-II′ activity at a K_i of 2.5 mM. Tyr284 conserved in family 7 enzymes is located in the cleft and binds to a sulfate ion. The molecular activity (V_{max}/K_m) of the mutant Y284F is significantly lower (300-fold) than that of the wild-type enzyme, although the Michaelis constants of both are comparable, suggesting that the mutant is more appropriate for structural analysis of the enzyme–substrate complex,[21] so we screened another crystallization condition for Y284F in the absence of any inhibitor. The Y284F crystals obtained in a mixture of calcium acetate, polyethylene glycol (PEG)-1000, and PEG-8000 were soaked in a trisaccharide (GGG or MMG) solution and used for X-ray data collection (Table 1). GGG and MMG-bound Y284F structures were finally refined at 1.65 Å and 1.55 Å resolution to *R*-factors of 18.8% and 16.7%, respectively (Fig. 3). No significant conformational change was seen among the ligand-free wild-type enzyme (PDB ID 2CWS) and trisaccharide-bound Y284F structures; the rmsd is low (0.21 Å) for all C^{α} atoms between the ligand-free wild-type enzyme and GGG or MMG-bound Y284F, since the trisaccharide-bound mutants have the two loops in the open form similar to the wild-type enzyme. In comparison to the crystal structure of N141C/N199C, the L1 loop in trisaccharide-bound Y284F moves into the opener position due to the accommodation of trisaccharides at the cleft. Both Y284F mutants complexed with GGG and MMG show the glove-like β-sandwich structures and bind trisaccharides to the cleft (Fig. 3c and d), indicating that the active site is located in the cleft. Positively charged residues arranged at the active site enable A1-II′ to bind to acidic alginate molecules (Fig. 3e and f). Loops L1 and L2 are arranged to surround the trisaccharides, GGG and MMG, which are bound to the mutant at subsites +1 to +3. The conformation of the unsaturated uronic acid was determined by calculating puckering parameters.[29] The puckering parameters of both unsaturated G and M are $Q = 0.47$ Å, $\Theta = 136°$, and $\Phi = 99°$. Unsaturated G and M adopt a half-chair ($^2H_1$) configuration; the C3, C4, and C5 atoms are on the plane as the result of a C4=C5 double bond. Unsaturated uronic acids were partially misfit with $F_o - F_c$ maps at subsite +1, revealing that alternative ligands like saturated uronic acids are accommodated at subsite +1. The trisaccharides prepared probably include both unsaturated and saturated saccharides because of their preparation through acid hydrolysis and lyase treatment. The ratio of the unsaturated and saturated uronic acid was calculated on the basis of conformational difference (Supplementary Data Fig. 1) with SHELXL programs.[30]

The Y284F–GGG complex consists of 226 amino acid residues, 214 water molecules, a glycerol molecule, and a trisaccharide GGG molecule that has unsaturated ($^2H_1$ configuration, 65%) and saturated ($^4C_1$ configuration, 35%) saccharides at the subsite +1 (Fig. 3a). The Y284F-MMG complex consists of 227 amino acid residues, 277 water molecules, a glycerol molecule, and a trisaccharide MMG molecule that has unsaturated (45%) and saturated ($^1C_4$ configuration, 55%) saccharides at subsite +1 (Fig. 3b).

Interactions between enzyme and trisaccharide

Interactions between Y284F mutant and trisaccharides through hydrogen bonds are shown in Fig. 4. Residues responsible for trisaccharide binding are located on strands SA2, SA3, SA4, SA5 and the loops (L1 and L2) over the cleft (Fig. 3c and d).

Both unsaturated and saturated saccharides in GGG or MMG-bound Y284F are accommodated at subsite +1 (Fig. 4c). Unsaturated saccharides are recognized by common residues Arg146, Gln189, His191, and Asn199 in both GGG and MMG-bound structures. A slight difference exists in the recognition profile of mutants between saturated and unsaturated saccharides. O62 of saturated saccharides is bound to Gln189, while no interaction between mutants and O62 of unsaturated saccharides is observed. Both carboxyl groups O61 and O62 of saturated G and M are recognized at subsite +1 by specific residues such as Arg146 and Gln189, while a difference exists in the binding mode of the mutant between saturated G and M at the subsite +1. O3 of saturated G is bound to His191 and Asn199, whereas O2 of saturated M is bound to His191 and Asn199.

At subsite +2, G and M are recognized by residues on SA2, SA4, and L1 (Fig. 4d). In the case of G, O61 is recognized by Thr139 and Asn141, O62 by Asn141, O3 by Gln97, and O2 by Tyr278 and Lys280. In the

Fig. 4. Active site structure (stereo diagram). (a) The interactions between amino acids and GGG., which is shown as a blue stick model. Residues colored green bind to the trisaccharide through hydrogen bonds (broken lines). (b) Interactions between amino acids and MMG., which is shown as a stick model (blue, G; red, M). Residues colored green bind to the trisaccharide through hydrogen bonds (broken lines). (c) Binding mode at subsite +1; the GGG- and MMG-bound Y284F structures are superimposed. Blue, G; red, M. Hydrogen bonds are indicated by dotted lines. (d) Binding mode at subsite +2; the GGG- and MMG-bound Y284F structures are superimposed. Blue, G; red, M. Hydrogen bonds are indicated by dotted lines. These pictures were drawn with MolFeat (FiatLux).

case of M, O61 is recognized by Thr139 and Asn141, O62 by Asn141, O4 by His191, O3 by Arg146 and Lys280, and O2 by Gln97 and Lys280.

At subsite +3, G is accommodated in both trisaccharide-bound structures, and recognized by residues on SA2 and SA3. O61 is recognized by Lys95

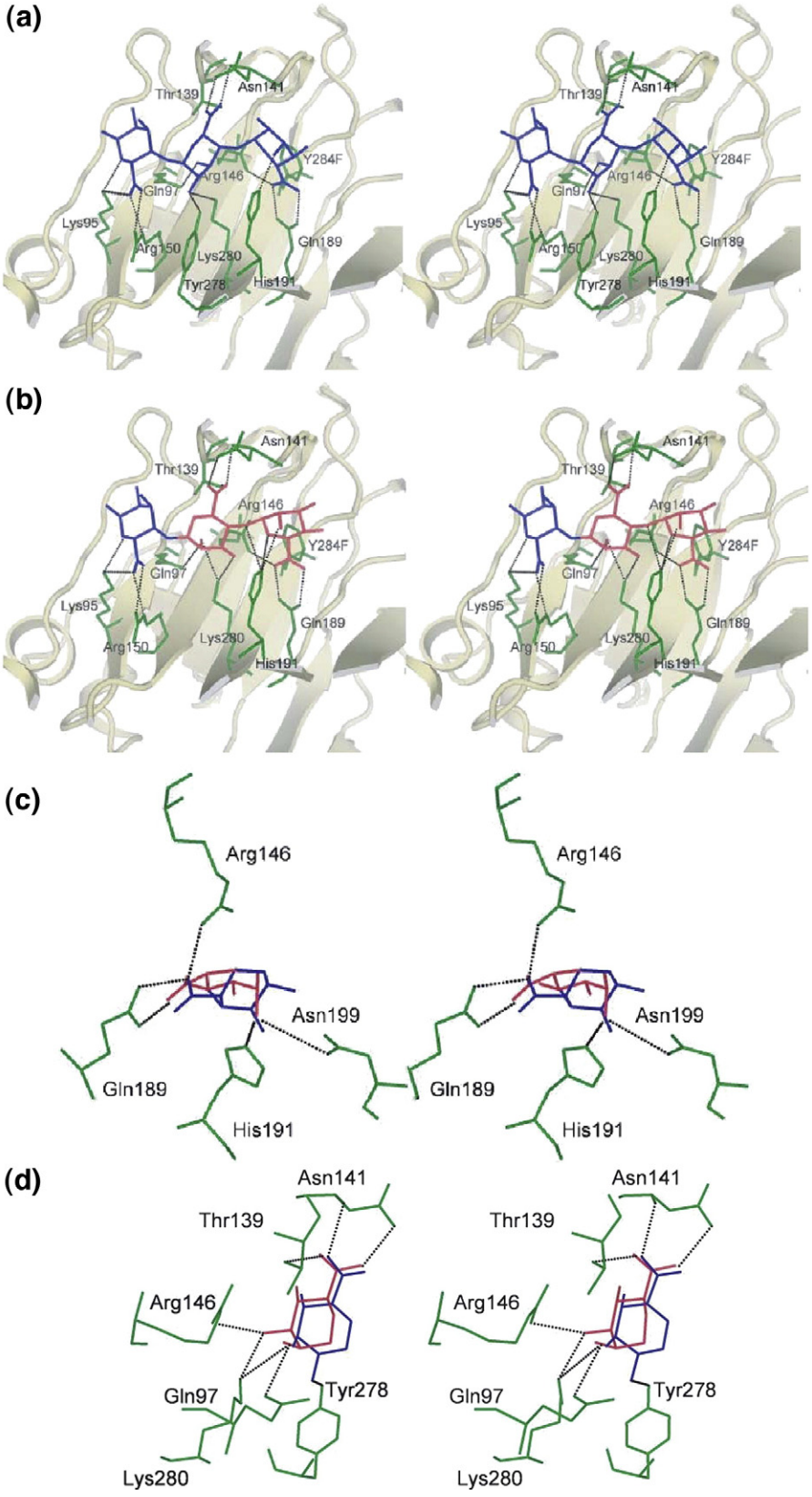

Fig. 4 (*legend on previous page*)

and Arg150, O62 by Arg150, and O5 and O4 by Gln97.

Structural determinants for A1-II′ broad substrate specificity

Alginate lyase A1-II′ acts on all regions of alginate molecules, i.e. poly(G), poly(M), and poly (MG), suggesting that the enzyme has an active site with binding ability to both G and M. The GGG- and MMG-bound Y284F structures were compared to clarify structural determinants for broad substrate specificity (Fig. 4). Since unsaturated G and M have identical configurations (α- and $^2H_1$ half-chair), we focused on interactions between the mutant and saturated saccharides bound at subsites +1 and +2. Arg146 and Gln189 bind to carboxyl groups O61 and O62 of both saccharides G and M bound at subsite +1, while His191 and Asn199 recognize their different hydroxyl groups, O3 of G and O2 of M (Fig. 4c). Also at subsite +2, Thr139 and Asn141 bind to carboxyl groups of both G and M (Fig. 4d). Gln97 and Lys280 recognize their different hydroxyl groups, O3 of G and O2 of M. Tyr278 interacts only with O2 of G.

On the basis of the above results, substrate carboxyl groups were found to be recognized by specific residues Arg146 and Gln189 at subsite +1; Thr139 and Asn141 at subsite +2; Lys95 and Arg150 at subsite +3. O3 of G and O2 of M are located at almost the same position and therefore recognized by residues such as His191 and Asn199 at subsite +1, and Gln97 and Lys280 at subsite +2. That is, A1-II′ strictly recognizes substrate carboxyl groups by specific residues, but interacts appropriately with substrate hydroxyl groups. These structural characteristics at the active site are probably involved in the broad substrate specificity of A1-II′.

Other than A1-II′ among alginate lyases structurally analyzed thus far, *Pseudoalteromonas* sp. alginate lyase (AALyase), a member of family 18, acts on all regions in alginate molecules, indicating broad substrate specificity.[31] As with family 7 alginate lyases, the enzyme adopts a β-sandwich structure as a basic fold (unpublished results; PDB ID 1J1T). Regarding the active cleft (SA2, SA3, SA4, and SA5), A1-II′ and AALyase (PDB ID 1J1T) are superimposed with a rmsd of 0.38 Å for 24 C^α atoms. A1-II′ residues responsible for trisaccharide binding such as Thr139, Asn141, Arg146, Arg150, Gln189, His191, Tyr278, and Lys280 are well conserved in AALyase, and the arrangement of these residues in crystal structures is almost identical for A1-II′ and AALyase, suggesting that this substrate recognition common to A1-II′ and AALyase is essential for broad substrate specificity.

Crystal structure of tetrasaccharide-bound H191N/Y284F

Arg146, Gln189, His191, and Tyr284 of A1-II′ are suspected of forming a catalytic site, since the molecular activity of their mutants is very low.[21] To identify catalytic residues, we analyzed the structure of the double mutant H191N/Y284F complexed with a substrate (tetrasaccharide). The refinement statistics are given in Table 1. The structure of GGMG-bound H191N/Y284F was finally refined at 1.8 Å resolution to an *R*-factor of 16.9%. The H191N/Y284F-GGMG complex consists of 232 amino acid residues, 151 water molecules, a glycerol molecule, and a tetrasaccharide molecule. The rmsd is 0.42 Å for 228 C^α atoms *versus* the ligand-free wild-type enzyme (PDB ID 2CWS), suggesting that there is no significant conformational change between the wild-type and mutant enzymes. The mutant also maintains the glove-like β-sandwich structure and accommodates tetrasaccharide in the active cleft. Unsaturated uronic acid is bound at subsite -1. Subsite +2 contains a mixture of G (40%) and M (60%) (Fig. 5a). Tetrasaccharide is thus regarded as GGMG with unsaturated G at the nonreducing terminus, and bound at subsites −1, +1, +2, and +3 in that order. Interactions at subsite −1 between the mutant and tetrasaccharide are as follows: O61-Lys218N^ζ, 3.3 Å; O62-Lys218N^ζ, 2.7 Å; O62-Lys205N^ζ, 2.7 Å; O3-Gln286$O^{\varepsilon1}$, 2.7 Å. Lys218, Lys205, and Gln286 are located on strands SA7, SA6, and a coil region between strands SA5 and SB3. The binding profile of the mutant to saccharide at subsites +1 to +3 is identical with that of trisaccharide-bound Y284F except for His191, which is replaced by Asn in the tetrasaccharide-bound mutant.

Possible catalytic reaction

The catalytic reaction of polysaccharide lyases has a three-step mechanism:[32] (i) removal or neutralization of the negative charge on the C6 carboxylate anion by A.A.1; (ii) abstraction of the C5 proton at subsite +1 by a general base (A.A.2); and (iii) proton donation to the O4 atom at subsite +1 by a general acid (A.A.3). In the H191N/Y284F-GGMG complex, distances at subsite +1 between carboxylate (O61 and O62) and Gln189 side chain ($N^{\varepsilon2}$ and $O^{\varepsilon2}$) are close enough for Gln189 to neutralize carboxylate anions. To identify A.A.2 and A.A.3 in the reaction of A1-II′, we calculated energy minimization with a CNS program[33] after *in silico* reverting Asn191 and Phe284 with His191 and Tyr284. In the reverted model, His191$N^{\varepsilon2}$ and Tyr284O^η approach C5 and O4 up to 3.3 Å and 3.2 Å (Fig. 5b). These results suggest that Gln189, His191, and Tyr284 function as catalysts A.A.1, A.A.2, and A.A.3, respectively.

Based on the crystal structures of A1-II′ in complex with alginate tri- or tetrasaccharide, Arg146 and Gln189 are candidates for A.A.1. The A1-II′ mutant Q189A with Gln189 to Ala significantly decreases its molecular activity (V_{max}/K_m) in comparison with the mutant R146A with Arg146 to Ala,[21] indicating that Gln189 plays a major role in neutralizing carboxylate anions of substrates. The function of Gln189 in family 7 A1-II′ is similar to that of Asn as A.A.1 in family 8 lyases for chondroitin,[26] xanthan,[34] and hyaluronate.[35]

Although, in the H191N/Y284F-GGMG complex, no residue is close enough to C5 and O4, His191 is a

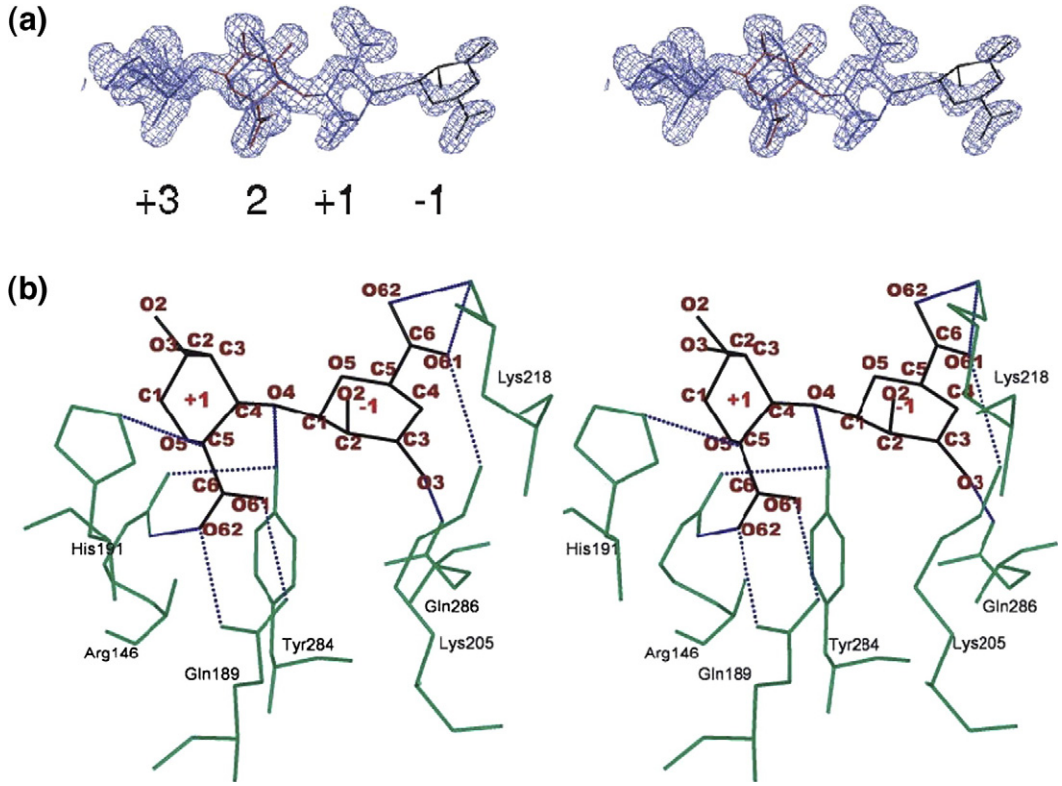

Fig. 5. Structure of tetrasaccharide-bound H191N/Y284F (stereo diagram). (a) The $F_o - F_c$ omit map for GGMG (blue, contoured at 3.0 σ). The tetrasaccharide is shown as a stick model (blue, G; red, M; black, unsaturated uronic acid). Numbers indicate the position of the subsite. (b) Energy-minimized model of wild-type A1-II′ and the tetrasaccharide (stereo diagram). Saccharides bound at subsites −1 and +1 are indicated as black stick models. Hydrogen bonds between the enzyme and saccharides are represented as broken lines. These pictures were drawn with Pymol (http://www.pymol.org) and MolFeat (FiatLux).

sole candidate for A.A.2 to be situated almost collinearly with the C5 proton of the saccharide bound at subsite +1 in the reverted model (Fig. 5b). This suggests that His191 abstracts the C5 proton. To function as an acid catalyst (A.A.3) for donation of a proton, Tyr284 is required to lower the pK_a of its side chain. Interaction of Tyr284O$^{\eta}$ and Arg146N$^{\eta}$ contributes to highly modulating pK_a of the side chain of Tyr284.

The candidates for A.A.2 and A.A.3 in family 7 alginate lyase A1-II′ differ from those in family 5 alginate lyase A1-III, although both cleave glycosidic bonds in alginate molecules through a β-elimination reaction. Structural analysis of A1-III complexed with MMM postulates that Arg239 functions as A.A.1 and Tyr246 as both A.A.2 and A.A.3.[20] In the reaction of A1-III, the nucleophilic side chain of Tyr246 abstracts the C5 proton and subsequently donates the proton to O4. A single tyrosine residue acting as base and acid catalysts is observed in family 5 and family 8 polysaccharide lyases.[20,26,34] In the reaction of family 8 chondroitin AC lyase, Asn183 functions as A.A.1 and Tyr242 as both A.A.2 and A.A.3.[26] Family 5 and family 8 lyases have a common basic scaffold (α/α-barrel) as a catalytic domain, and catalytically important residues are superimposed between family 5 A1-III and family 8 xanthan lyase.[34] Since, distinct from α/α-barrel A1-III, A1-II′ adopts β-sandwich as a basic scaffold, there might be a diversity in catalytic residues between A1-II′ and A1-III.

In order to clarify the intrinsic function of residues in the active cleft, we are now studying the reaction mechanism of A1-II′ and A1-III through X-ray crystallographic and mutational analyses.

Conclusions

A1-II′ has an active site in the cleft covered with two flexible loops. The flexibility in loops is essential for substrate binding, i.e. accommodation of substrates in the active site. Both G and M in alginate molecules are bound to the active site; the enzyme interacts appropriately with substrate hydroxyl groups, although substrate carboxyl groups are recognized by specific residues, and these structural characteristics provide A1-II′ with broad substrate specificity. Regarding catalytic residues interacting with the saccharide bound at subsite +1, we postulate that Gln189 neutralizes the negative charge of the carboxyl group, His191 abstracts the C5 proton, and Tyr284 donates the proton to the glycoside bond to be cleaved. This is, to our knowledge, the first report of the structure and function relationship of family 7 polysaccharide lyases.

Materials and Methods

Materials

Sodium alginate (average molecular mass, 26 kDa; M/G ratio, 56.5/43.5) from *Eisenia bicyclis* was purchased from Nacalai Tesque. The HisTrap™ HP column (2 cm × 5 cm) and the Q Sepharose High Performance 16/20 column were from GE Healthcare Bio-Science. The primers for site-directed mutagenesis were from Hokkaido System Science; and the Quick Change site-directed mutagenesis kit was from Stratagene.

Alginate oligosaccharides were prepared from sodium alginate through partial hydrolysis and separation into G-rich, M-rich, and mixed MG blocks.[36,37] A G-rich or M-rich block (each 100 mg) was digested at 30 °C for 24 h by A1-II′ (200 μg) in 40 ml of 20 mM Tris–HCl (pH 7.5). The resulting oligosaccharides were applied onto a Q Sepharose High Performance 16/20 column previously equilibrated with 50 mM ammonium bicarbonate, and eluted with a linear gradient of 50 mM–500 mM ammonium bicarbonate. Tri- and tetrasaccharides were recovered from each block by monitoring the absorbance at 235 nm owing to the C=C double bond of unsaturated uronic acids, and validated by thin layer chromatography to be almost homogeneous as described.[16] As described in Results and Discussion, trisaccharides, GGG and MMG, include saturated as well as unsaturated uronic acids at the nonreducing terminus due to their preparation through acid hydrolysis and the successive lyase treatment.

Computational analysis

Based on the primary structure of A1-II′ (accession number AB120939), its disordered regions were predicted by a GlobPlot program†.[24] MD simulation was conducted by a GROMACS program‡.[25] using the crystal structure of ligand-free A1-II′ (PDB ID 2Z42) as a starting model. After removing all sulfate ions and water molecules from the crystal structure, the protein and water molecules were freshly loaded into a calculation box (30 nm × 30 nm × 30 nm). Energy in the box including the protein and water molecules was minimized (0.001 ps × 1000 steps). After protein-restrained MD calculation (0.001 ps × 1000 steps), full MD calculation (0.002 ps × 500,000 steps) was carried out.

Site-directed mutagenesis, protein expression and purification

To introduce mutations in Asn141 and Asn199 with Cys for expression of a double mutant N141C/N199C, two pairs of primers were designed as follows.

N141C sense:
GTGGCACGACGGCCTGCAGCAGTTACCCG
N141C antisense:
CGGGTAACTGCTGCAGGCCGTCGTGCCAC
N199C sense:
GATGCAGGCACTTGTGCACCGCCGCTGGTC
N199C antisense:
GACCAGCGGCGGTGCACAAGTGCCTGCATC

To introduce mutations in His191 and Tyr284 with Asn and Phe for expression of the double mutant H191N/Y284F, two pairs of primers were designed as follows.

H191N sense:
CATCGTGGCGCAGATTAACGGCATCATGG
H191N antisense:
CCATGATGCCGTTAATCTGCGCCACGATG
Y284F sense:
CAAGGCTGGCCAACTTCGTTCAGGACAACACGTCG
Y284F antisense:
CGACGTGTTGTCCTGAACGAAGTTGGCCAGCCTTG.

Underlining in the oligonucleotide sequences indicates the position of mutations. Site-directed mutagenesis was conducted using plasmid pET21b-A1-II′(S)[16] as a template and the synthetic oligonucleotides as sense and antisense primers according to the manufacturer's directions for the Quick Change site-directed mutagenesis kit. Resultant plasmids were designated as pET21b-A1-II′(N141C/N199C) and pET21b-A1-II′(H191N/Y284F). Mutations were confirmed by DNA sequencing (Shimadzu Genomic Research Center).

Cells of *Escherichia coli* host strain BL21(DE3) were transformed with the plasmid pET21b-A1-II′(N141C/N199C), or pET21b-A1-II′(Y284F),[21] or pET21b-A1-II′(H191N/Y284F). *E. coli* transformants for expression of N141C/N199C, Y284F, or H191N/Y284F were cultivated as described.[38] Unless otherwise specified, all purification was done at 0–4 °C. A1-II′ and its mutants were expressed as a fusion protein-tagged C-terminal histidine sequence (−LEHHHHHH). *E. coli* cells harboring plasmids were grown in Luria-Bertani medium, collected by centrifugation at 6000*g* for 5 min at 4 °C, washed with buffer A (20 mM Tris–HCl, pH 7.5), then resuspended in the same buffer.[38] Cells were disrupted ultrasonically (Insonator model 201 M, Kubota) at 0 °C and 9 kHz for 20 min, and the clear solution obtained by centrifugation at 20,000*g* for 20 min at 4 °C was used as the cell extract. The cell extract was fractionated with ammonium sulfate. The precipitate (0–15% saturation) was removed by centrifugation at 20,000*g* for 20 min at 4 °C. The supernatant containing A1-II′ was dialyzed against buffer A. The enzyme solution was applied to Q Sepharose High Performance 16/20 column previously equilibrated with buffer A. The enzyme was eluted with buffer A (flow-through). The enzyme solution was dialyzed against buffer B (20 mM imidazole, 0.5 M NaCl, 20 mM Tris–HCl, pH 7.5), then applied to a nickel-bound HisTrap™ HP column previously equilibrated with buffer B. The enzyme was eluted with a linear gradient of imidazole (20 mM–250 mM) in 0.5 M NaCl, 20 mM Tris–HCl (pH 7.5). Enzyme fractions eluted with 200 mM imidazole were dialyzed against 5 mM Tris-HCl (pH 7.5) and used as a purified enzyme source. In the case of N141C/N199C, buffers used in purification procedures included DTT at a final concentration of 0.5 mM. Purified enzymes were concentrated by ultrafiltration with Centriprep (Millipore) for crystallization.

Crystallization and modeling

Distinct from the crystallization condition described previously,[38] the wild-type enzyme was also crystallized under other conditions (10 mg/ml enzyme, 0.1 M 2-(*N*-morpholino)ethanesulfonic acid–NaOH (pH 6.5), 2.0 M ammonium sulfate, 5% PEG-400). Its crystal structure has a hydrogen bond between Asn141 and Asn199 (loop-closed form). N141C/N199C was crystallized under the same conditions as the wild-type enzyme in the previous

† http://globplot.embl.de/
‡ http://www.gromacs.org/

report; 10 mg/ml N141C/N199C, 0.1 M sodium acetate (pH 4.5), 0.2 M ammonium sulfate, 27.5% PEG-8000.[38] The crystallization conditions of Y284F were screened by using commercial crystallization kits from Hampton Research (Laguna Niguel) in 96-well Intelli-plates (Art Robbins Instruments). Y284F was crystallized with calcium acetate, PEG-1000, and PEG-8000 as the major precipitant. After improvement, the precipitant solution most suitable for Y284F crystallization was determined to consist of 15 mg/ml Y284F, 50 mM sodium acetate (pH 5.0), 0.2 M calcium acetate, 10% PEG-1000, 15% PEG-8000. Crystallization of H191N/Y284F was also attempted under a large number of conditions with calcium chloride and PEG-4000 as the major precipitant. After improvement, the precipitant solution most suitable for H191N/Y284F crystallization was determined to consist of 10 mg/ml H191N/Y284F, 50 mM 4-(2-hydroxyethyl)-1-piperazineethanesulfonic acid (Hepes)–NaOH (pH 7.5), 0.2 M calcium chloride, 25% PEG-4000.

The N141C/N199C crystal was soaked in 0.1 M sodium acetate (pH 4.5), 0.2 M ammonium sulfate, 35% PEG-8000 for cryoprotection. Diffraction data were collected in a resolution range of 50–2.1 Å. The Y284F crystal was soaked at 20 °C for 30 min in 50 mM Hepes–NaOH (pH 8.0), 10% PEG-1000, 10% PEG-8000 containing 50 mM trisaccharide derived from the G-rich block (G3-solution), then in G3-solution supplemented with 20% (v/v) glycerol for cryoprotection. Diffraction data were collected in a resolution range of 50–1.65 Å. Another crystal of Y284F was soaked at 20 °C for 30 min in 50 mM Hepes–NaOH (pH 8.0), 10% PEG-1000, 10% PEG-8000 containing 50 mM trisaccharide derived from the M-rich block (M3-solution), and in M3-solution supplemented with 20% glycerol for cryoprotection. The diffraction data were collected in a resolution range of 50–1.50 Å. The H191N/Y284F crystal was soaked at 20 °C for 30 min in 50 mM Hepes–NaOH (pH 8.0) and 20% PEG-4000 containing 50 mM tetrasaccharide derived from the G-rich block (G4-solution), then in G4-solution supplemented with 20% glycerol for cryoprotection. The diffraction data were collected in a resolution range of 50–1.80 Å. All diffraction data were collected from synchrotron radiation of wavelength 1.0 Å at the BL-38B1 station of SPring-8, Hyogo, Japan. The data were processed, merged, and scaled using the HKL2000 program package (DENZO and SCALEPACK).[39] Crystal structures of ligand-free or bound A1-II′ mutants were determined by molecular replacement with the coordinates of the ligand-free wild-type enzyme as an initial model (PDB ID 2CWS). Structural models were refined with CNS programs.[33] Parameter and topology files of G and M were prepared at the PRODRG site using the model coordinate§. Unsaturated uronic acids were partially misfit with the F_o-F_c maps, revealing that saturated uronic acid, which was derived through acid hydrolysis or from nonreducing side in lyase reaction, was included in the trisaccharide. The ratio of unsaturated and saturated uronic acids was calculated using a SHELXL program based on the conformational difference as α-L-guluronate, β-D-mannuronate, and unsaturated uronic acid take $^4C_1$, $^1C_4$, and $^2H_1$ configurations, respectively (Supplemental Fig. 1).[30] After each cycle of refinement, models were adjusted manually and improved using TURBO-FRODO (AFMB-CNRS). The final quality of models was assessed by PROCHECK.[40] Subsite numbers were determined according to definition by Davies *et al*. as follows: subsites are usually labeled so that −n represents the nonreducing end and +n the reducing end, and cleavage occurs between −1 and +1 sites.[41]

Asn191 and Phe284 in tetrasaccharide-bound H191N/Y284F were manually reverted to His and Tyr with TURBO-FRODO. The reverted model (tetrasaccharide-bound wild-type) was constructed after energy minimization calculation for 100 cycles using a CNS program.[33]

Assays for N141C/N199C

To determine the thiol group, DTNB was dissolved in 50 mM potassium phosphate (pH 7.5) at the concentration of 1 mg/ml. Sample solutions (1 ml) containing N141C/N199C at various concentrations of 0.2, 0.4, 0.8, and 1.6 mg/ml were reacted with the DTNB solutions (100 ml) at 25 °C. The increase of absorbance at 412 nm due to the formation of 2-nitro-5-thiobenzonate dianion in the mixture was monitored.[28] The thiol group content in the reaction mixture was determined with DTT as a standard.

To examine the rigidity of protein structure, the transition temperature of wild-type and mutant (N141C/N199C) enzymes was determined by DSC with a calorimeter (Microcal MC-2 ultrasensitive microcalorimeter, MicroCal LLC.). Purified wild-type and mutant enzymes were dialyzed against 5 mM sodium phosphate (pH 6.5) in the presence or absence of 0.5 mM DTT.

For enzyme assay, the mutant enzyme (N141C/N199C) was incubated at 30 °C in a reaction mixture (1 ml) consisting of sodium alginate and 50 mM Tris-HCl (pH 7.5). Enzyme activity in the presence of different substrate concentrations (0.01, 0.03, 0.05, 0.07, 0.1, 0.2, 0.3, 0.4, 0.5, 0.6, 0.8, 1.0, 1.5, and 2.0 mg/ml) was measured by monitoring the increase in absorbance at 235 nm. One unit (U) of enzyme activity was defined as the amount of enzyme required to produce an increase of 1.0 in absorbance at 235 nm per min. Protein content was determined by the method of Bradford, with bovine serum albumin as the standard,[42] or by measuring the absorbance at 280 nm assuming that $E_{280}=1.0$ corresponds to 0.85 mg/ml. Kinetic parameters K_m and V_{max} were calculated with the Michaelis-Menten plot using KaleidaGraph software (Synergy Software).

Protein Data Bank accession number

The atomic coordinates and protein factors have been deposited in the Protein Data Bank as entries 2Z42 for wild-type in loop-closed form, 2ZA9 for ligand-free N141C/N199C, 2ZAB for GGG-bound Y284F, 2ZAC for MMG-bound Y284F, and 2ZAA for GGMG-bound H191N/Y284F.

§ http://davapc1.bioch.dundee.ac.uk/programs/prodrg

Acknowledgements

We thank the Japan Synchrotron Radiation Research Institute (JASRI) and especially Drs K. Hasegawa and H. Sakai for their help in collecting X-ray data at beamline BL38B1 of SPring-8. X-ray diffraction data was collected at BL38B1 of SPring-8 under the approval of JASRI. This work was supported, in part, by Research Fellowships from

the Japan Society for the Promotion of Science for Young Scientists (to K.O.) and by Grants-in-Aid (to W. H., B.M., and K.M.) and Targeted Proteins Research Program (to W.H., B.M., and K.M.) from the Ministry of Education, Culture, Sports, Science, and Technology of Japan.

Supplementary Data

Supplementary data associated with this article can be found, in the online version, at doi:10.1016/j.jmb.2008.05.008

References

1. Gacesa, P. (1988). Alginates. *Carbohydr. Polym.* **8**, 161–182.
2. May, T. B. & Chakrabarty, A. M. (1994). *Pseudomonas aeruginosa*: genes and enzymes of alginate synthesis. *Trends Microbiol.* **2**, 151–157.
3. Schweizer, H. P. & Boring, J. R. (1973). Antiphagocytic effect of slime from a mucoid strain of *Pseudomonas aeruginosa*. *Infect. Immun.* **3**, 762–767.
4. Govan, J. R. W. & Deretic, V. (1996). Microbial pathogenesis in cystic fibrosis: mucoid *Pseudomonas aeruginosa* and *Burkholderia cepacia*. *Microbiol. Rev.* **60**, 539–574.
5. Remminghorst, U. & Rehm, B. H. (2006). Bacterial alginates: from biosynthesis to applications. *Biotechnol. Lett.* **28**, 1701–1712.
6. Onsøyen, E. (1996). Commercial applications of alginates. *Carbohydr. Eur.* **14**, 26–31.
7. Akiyama, H., Endo, T., Nakakita, R., Murata, K., Yonemoto, Y. & Okayama, K. (1992). Effect of depolymerized alginates on the growth of bifidobacteria. *Biosci. Biotechnol. Biochem.* **56**, 355–356.
8. Iwamoto, M., Kurachi, M., Nakashima, T., Kim, D., Yamaguchi, K., Oda, T. *et al.* (2005). Structure-activity relationship of alginate oligosaccharides in the induction of cytokine production from RAW264.7 cells. *FEBS Lett.* **579**, 4423–4429.
9. Iwamoto, Y., Xu, X., Tamura, T., Oda, T. & Muramatsu, T. (2003). Enzymatically depolymerized alginate oligomers that cause cytotoxic cytokine production in human mononuclear cells. *Biosci. Biotechnol. Biochem.* **67**, 258–263.
10. Kawada, A., Hiura, N., Shiraiwa, M., Tajima, S., Hiruma, M., Hara, K. *et al.* (1997). Stimulation of human keratinocyte growth by alginate oligosaccharides, a possible co-factor for epidermal growth factor in cell culture. *FEBS Lett.* **408**, 43–46.
11. Kawada, A., Hiura, N., Tajima, S. & Takahara, H. (1999). Alginate oligosaccharides stimulate VEGF-mediated growth and migration of human endothelial cells. *Arch. Dermatol. Res.* **291**, 542–547.
12. Kurachi, M., Nakashima, T., Miyajima, C., Iwamoto, Y., Muramatsu, T., Yamaguchi, K. & Oda, T. (2005). Comparison of the activities of various alginates to induce TNF-α secretion in RAW264.7 cells. *J. Infect. Chemother.* **11**, 199–203.
13. Wong, T. Y., Preston, L. A. & Schiller, N. L. (2000). Alginate lyase: review of major sources and enzyme characteristics, structure-function analysis, biological roles, and applications. *Annu. Rev. Microbiol.* **54**, 289–340.
14. Hisano, T., Yonemoto, Y., Yamashita, T., Fukuda, Y., Kimura, A. & Murata, K. (1995). Direct uptake of alginate molecules through a pit on the bacterial cell surface: a novel mechanism for the uptake of macromolecules. *J. Ferment. Bioeng.* **79**, 538–544.
15. Hashimoto, W., Momma, K., Maruyama, Y., Yamasaki, M., Mikami, B. & Murata, K. (2005). Structure and function of bacterial super-biosystem responsible for import and depolymerization of macromolecules. *Biosci. Biotechnol. Biochem.* **69**, 673–692.
16. Miyake, O., Ochiai, A., Hashimoto, W. & Murata, K. (2004). Origin and diversity of alginate lyases of families PL-5 and -7 in *Sphingomonas* sp. strain A1. *J. Bacteriol.* **186**, 2891–2896.
17. Coutinho, P. M. & Henrissat, B. (1999). Carbohydrate-active enzymes: an integrated database approach. In (Gilbert, H. J., Davies, G., Henrissat, B. & Svensson, B., eds), pp. 3–12, The Royal Society of Chemistry, Cambridge, UK.
18. Yoon, H.-J., Mikami, B., Hashimoto, W. & Murata, K. (1999). Crystal structure of alginate lyase A1-III from *Sphingomonas* species A1 at 1.78 Å resolution. *J. Mol. Biol.* **290**, 505–514.
19. Mikami, B., Suzuki, S., Yoon, H.-J., Miyake, O., Hashimoto, W. & Murata, K. (2002). X-ray structural analysis of alginate lyase A1-III mutants/substrate complexes: activation of a catalytic tyrosine residue by a flexible lid loop. *Acta Crystallogr. A*, **58**, C271.
20. Yoon, H.-J., Hashimoto, W., Miyake, O., Murata, K. & Mikami, B. (2001). Crystal structure of alginate lyase A1-III complexed with a trisaccharide product at 2.0 Å resolution. *J. Mol. Biol.* **307**, 9–16.
21. Yamasaki, M., Ogura, K., Hashimoto, W., Mikami, B. & Murata, K. (2005). A structural basis for depolymerization of alginate by polysaccharide lyase family-7. *J. Mol. Biol.* **352**, 11–21.
22. Yamasaki, M., Moriwaki, S., Miyake, O., Hashimoto, W., Murata, K. & Mikami, B. (2004). Structure and function of a hypothetical *Pseudomonas aeruginosa* protein PA1167 classified into family PL-7: A novel alginate lyase with a β-sandwich fold. *J. Biol. Chem.* **279**, 31863–31872.
23. Osawa, T., Matsubara, Y., Muramatsu, T., Kimura, M. & Kakuta, Y. (2005). Crystal structure of the alginate (poly α-L-guluronate) lyase from *Corynebacterium* sp. at 1.2 Å resolution. *J. Mol. Biol.* **345**, 1111–1118.
24. Linding, R., Russell, R. B., Neduva, V. & Gibson, T. J. (2003). GlobPlot: Exploring protein sequences for globularity and disorder. *Nucleic Acids Res.* **31**, 3701–3708.
25. Lindahl, E., Hess, B. & van der Spoel, D. (2001). GROMACS 3.0: a package for molecular simulation and trajectory analysis. *J. Mol. Model.* **7**, 306–317.
26. Lunin, V. V., Li, Y., Linhardt, R. J., Miyazono, H., Kyogashima, M., Kaneko, T. *et al.* (2004). High-resolution crystal structure of *Arthrobacter aurescens* chondroitin AC lyase: an enzyme-substrate complex defines the catalytic mechanism. *J. Mol. Biol.* **337**, 367–386.
27. Jedrzejas, M. J., Mello, L. V., De Groot, B. L. & Li, S. (2002). Mechanism of hyaluronan degradation by *Streptococcus pneumoniae* hyaluronate lyase. Structures of complexes with the substrate. *J. Biol. Chem.* **277**, 28287–28297.
28. Riddle, P. W., Blakeley, R. L. & Zerner, B. (1979). Elleman's reagent: 5,5′-dithiobis(2-nitrobenzoic acid): a reexamination. *Anal. Biochem.* **94**, 75–81.
29. Cremer, D. & Pople, J. A. (1975). General definition of ring puckering coordinates. *J. Am. Chem. Soc.* **97**, 1354–1358.
30. Sheldrick, G. M. & Schneider, T. R. (1997). Shelxl: high-resolution refinement. *Methods Enzymol.* **277**, 319–343.

31. Iwamoto, Y., Iriyama, K., Osatomi, K., Oda, T. & Muramatsu, T. (2002). Primary structure and chemical modification of some amino acid residues of bifunctional alginate lyase from a marine bacterium *Pseudoalteromonas* sp. strain No. 272. *J. Protein Chem.* **21**, 453–461.
32. Linker, A., Meyer, K. & Hoffman, P. (1956). The production of unsaturated uronides by bacterial hyaluronidases. *J. Biol. Chem.* **219**, 13–25.
33. Brünger, A. T., Adams, P. D., Clore, G. M., DeLano, W. L., Gros, P., Grosse-Kunstleve, R. W. *et al.* (1998). Crystallography and NMR system (CNS): A new software system for macromolecular structure determination. *Acta Crystallogr. D*, **54**, 905–921.
34. Maruyama, Y., Hashimoto, W., Mikami, B. & Murata, K. (2005). Crystal structure of *Bacillus* sp. GL1 xanthan lyase complexed with a substrate: insights into the enzyme reaction mechanism. *J. Mol. Biol.* **350**, 974–986.
35. Li, S., Kelly, S. J., Lamani, E., Ferraroni, M. & Jedrzejas, M. J. (2000). Structural basis of hyaluronan degradation by *Streptococcus pneumoniae* hyaluronate lyase. *EMBO J.* **19**, 1228–1240.
36. Haug, A., Larsen, B. & Smidsrod, O. (1966). A study of the constitution of alginic acid by partial acid hydrolysis. *Acta Chem. Scand.* **20**, 183–190.
37. Smidsrod, O., Haug, A. & Larsen, B. (1966). The influence of pH on the rate of hydrolysis of acidic polysaccharides. *Acta Chem. Scand.* **20**, 1026–1034.
38. Yamasaki, M., Ogura, K., Moriwaki, S., Hashimoto, W., Murata, K. & Mikami, B. (2005). Crystallization and preliminary X-ray analysis of alginate lyases A1-II and A1-II′ from *Sphingomonas* sp. A1. *Acta Crystallogr. F*, **61**, 288–290.
39. Otwinowski, Z. & Minor, W. (1997). Processing of X-ray diffraction data collected in oscillation mode. *Methods Enzymol.* **276**, 307–326.
40. Laskowski, R. A., MacArthur, M. W., Moss, D. S. & Thornton, J. M. (1993). PROCHECK: a program to check the stereochemical quality of protein structures. *J. Appl. Crystallogr.* **26**, 283–291.
41. Davies, G. J., Wilson, K. S. & Henrissat, B. (1997). Nomenclature for sugar-binding subsites in glycosyl hydrolases. *Biochem. J.* **321**, 557–559.
42. Bradford, M. M. (1976). A rapid and sensitive method for the quantitation of microgram quantities of protein utilizing the principle of protein-dye binding. *Anal. Biochem.* **72**, 248–254.